Deep Optical Images of the Ejecta Nebula Around the Wolf-Rayet Star WR 8 (HD 62910)

ROBERT A. FESEN,¹ DANIEL PATNAUDE,² WEI-HAO WANG,³ YOU-HUA CHU,⁴ JASON SUN,⁵ MANUEL C. PEITSCH,⁶ MARTIN PUGH,⁷ SCOTT GARROD,⁷ MICHAEL SELBY,⁷ AND ALEX WORONOW⁸

¹6127 Wilder Lab, Department of Physics and Astronomy, Dartmouth College, Hanover, NH 03755 USA
 ²Smithsonian Astrophysical Observatory, MS-3, 60 Garden Street, Cambridge, MA 02138 USA
 ³Institute of Astronomy and Astrophysics, Academia Sinica (ASIAA), No. 1, Roosevelt Road, Taipei 10617, Taiwan, R.O.C.
 ⁴Department of Physics, National Sun Yet-Sen University, No. 70, Lienhai Rd., Kaohsiung 804201, Taiwan, R.O.C.
 ⁵Department of Physics, National Tsing Hua University, No. 101, Section 2, Kuang Fu Road, Hsinchu 30013, Taiwan, R.O.C.
 ⁶Roboscopes at e-EyE Entre Encinas y Estrellas Observatory, Camino de los Molinos 06340 Fregenal de la Sierra, Spain
 ⁷Observatorio El Sauce, Rio Hurtado, Coquimbo, Chile

⁸Department of Geosciences, University of Houston, 4800 Calhoun Rd. Houston, TX 77004 USA

ABSTRACT

We report the results of deep H α and [O III] images of the bright WN6/WC4 Wolf-Rayet star WR 8 (HD 62910). These data show considerably more surrounding nebulosity than seen in prior imaging. The brighter portions of the nebula span $\simeq 6'$ in diameter and exhibit considerable fine-scale structure including numerous emission clumps and bright head-tail like features presumably due to the effects of the WR star's stellar winds. Due to the overlap of a relatively bright band of unrelated foreground diffuse interstellar H α emission, WR 8's nebula is best viewed via its [O III] emission. A faint 9' × 13' diffuse outer nebulosity is detected surrounding the nebula's main ring of emission. Comparison of the nebula's optical structure with that seen in WISE 22 μ m data shows a similarly clumpy structure but within a better defined emission shell of thermal continuum from dust. The infrared shell is coincident with the nebula's southern [O III] emissions but is mainly seen in the fainter outer portions of the northern [O III] emission clumps. It is this greater radial distance of dust emission in the nebula's northern areas that leads to a striking off-center position of the WR star from the IR shell.

Keywords: ISM: Emission Nebula - Early-Type Emission Stars: Wolf-Rayet Stars

1. INTRODUCTION

Wolf-Rayet (WR) stars are thought to be the helium-burning descendants of a galaxy's most massive stars with initial masses $\geq 30~\rm M_{\odot}$ (Maeder & Conti 1994; Conti 2000; Crowther 2008). Identified by their broad optical line emissions, these stars have stellar winds characterized by terminal velocities ranging from 1000 to 4000 km s⁻¹ and due to their very high luminosities undergo high mass-loss rates $\sim 10^{-5}~\rm M_{\odot}~\rm yr^{-1}$ (Hamann et al. 2019; Sander et al. 2022). During its WR phase, a massive star can release up to $10^{51}~\rm erg$, which is comparable to that of a supernova (SN) explosion. Consequently, WR stars can have significant effects on their local environments (Abbott 1982; Oey 1999).

WR stars are categorized into two main subtypes based on the types of optical line emissions they exhibit; WN stars show emission lines from helium and nitrogen ions, while WC stars show carbon and oxygen lines in addition to helium lines. Emission lines of hydrogen are notably absent in all but a few WR stars, as are strong absorption lines (Abbott & Conti 1987). WR subtypes are also subdivided into an excitation/ionization sequence where the highest to lowest

excitation spectral features are denoted by low to high subclass numbers. Thus, WN stars are arranged WN3 to WN9 based on the relative strengths of N III, N IV, and N V lines. Similarly, WC stars have subtypes based on excitation/ionization differences, ranging from WC3 to WC9.

A few WR stars exhibit both WN and WC like spectra in that they show strong emission lines of carbon and nitrogen simultaneously (Conti & Massey 1989; Crowther 2007). It is unclear if such stars are single stars in the transition between WN and WC, or if some are cases of WN + WC binaries. Regardless, such stars are relatively rare, consistent with an expected short $\sim 10^4$ yr transition time-scale; see discussion in Hillier et al. (2021).

Due to their strong stellar winds and high mass loss rates, WR stars are often surrounded by optical emission arcs or nebula 'rings' (Chu 1981; Chu et al. 1983). Since the first Galactic WR nebulae were discovered in the 1960's (Johnson & Hogg 1965), dozens more have been identified (Chu 1991; Chu et al. 1983). WR associated nebulae are categorized into three groups based on their formation mechanisms. These are: W-type for a wind-blown ISM bubble, E-type for stellar mass ejec-

tion nebulae, and R-type for a radiatively excited H II region. Most WR nebula are associated with WN type stars, and WN8 stars in particular (Chu 2016).

Of special interest are the E-type ejecta WR star ring nebulae due to their formation by means of substantial and violent mass loss episodes in the recent history of the star's mass loss evolution. Unlike wind-blown (W) or H II region (R) types of WR ring nebulae, E-type ejecta nebula tend to more clumped and irregular in morphology (Chu 1981, 1991). These nebulae also show greater nitrogen and helium abundances relative to the ISM consistent with CNO cycle processed material (Kwitter 1984; Esteban et al. 2016).

The eighth WR star listed in the well referenced van der Hucht (2001) catalog of Wolf-Rayet stars is the WR star HD 62910 (V = 10.1 mag), hence giving it the WR 8 identification. Located in the southern hemisphere constellation of Puppis, it lies at an estimated distance of 3.52 ± 0.16 kpc (Bailer-Jones et al. 2021). It has been classified as a WN6/WC4 due to its spectrum showing both WN and WC spectral features (van der Hucht et al. 1981; Willis & Stickland 1990).

Some WN/WC stars, such as WR 145 and WR 153, are known to be spectroscopic binaries, and there are indications that WR 8 might also be a binary. While Niemela (1991) and Marchenko et al. (1998) found strong evidence for WR 8's binary nature, Willis & Stickland (1990) found a good correlation of line widths and excitation potential for both WN and WC spectral features suggesting they formed in a single stellar wind. Although a single star conclusion was supported by Deshmukh et al. (2024), their instrument's resolution may not have been sufficient to rule out the binary nature of WR 8 and Sander et al. (2012) was unable to fit its spectrum using a single-star model.

Despite several searches looking for a nebula associated with WR 8 (e.g., Heckathorn et al. 1982; Chu et al. 1983; Marston et al. 1994a), a faint and clumpy nebulosity was only recently discovered by Stock & Barlow (2010) (see Fig. 1) examining the 1.2 m Schmidt AAS/UKST SuperCOSMOS H α survey images of the southern galactic plane also known as the Southern H α Survey or SHS (Parker et al. 2005). Due to the nebula's highly clumpy appearance, the WR 8 nebula was classified as an E or ejecta type WR ring nebula (Stock & Barlow 2010; Stock et al. 2011), thus a member of the rarer type of WR nebulae.

A nebula around WR 8 was independently detected by Wachter et al. (2011) in the infrared from an inspection of WISE 22 μ m images. Subsequent optical and infrared spectra showed enhanced nitrogen abundance (Stock et al. 2011; Stock & Barlow 2014) characteristic of material lost following the star's red supergiant (RSG) or luminous blue variable (LBV) phase and consistent with its E-type ejecta WR subtype. Infrared 22 μ m WISE images of WR 8's nebula shows a nearly complete ring of emission 5.3' in diameter but one that is centered

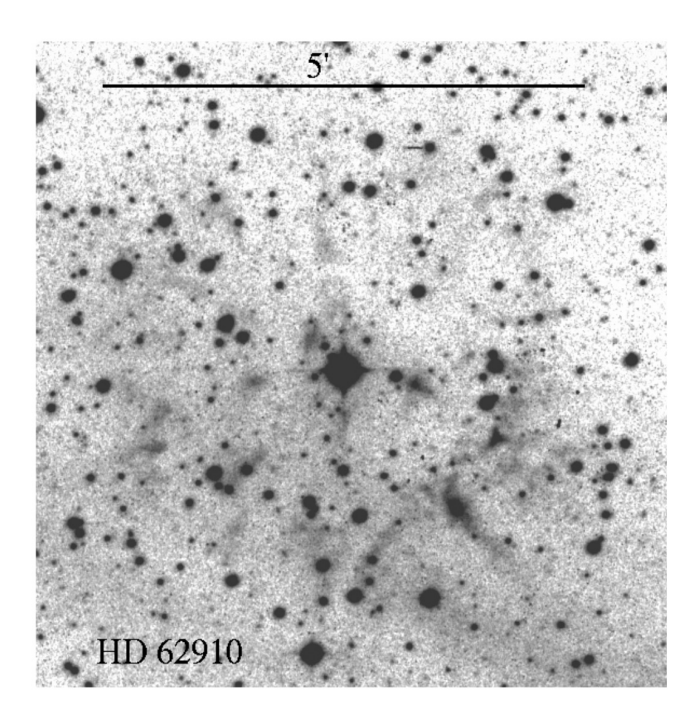


Figure 1. Discovery H α image showing faint nebulosity around and in front of WR 8 (from Stock & Barlow 2010).

almost an arcminute north of the WR star (Toalá et al. 2015).

Here we report the results of deep ${\rm H}\alpha$ and [O III] images of the Wolf-Rayet star WR 8 which reveal the nebula in far greater detail than seen in prior published images. These images reveal a complex nebula composed of emission clumps and radially aligned streamers plus a faint outer emission halo in [O III] emission. Our observations are described in §2 with results and discussion presented in §3.

2. OBSERVATIONS

Due to the absence of any published $H\alpha$ images of WR 8 since the 2010 discovery of its associated nebula (Stock & Barlow 2010; Fig. 1), plus the lack of any [O III] images of this WR nebula, exploratory images of WR 8 were obtained in December 2023 using a 0.5 m Planewave CDK20 f/6.8 telescope at the Yushan National Park in Chia-Yi, Taiwan. A series of $90 \times 480 \text{ s}$ exposures in both $H\alpha + [N II] \lambda\lambda6548,6583$ and [O III] $\lambda 5007$ filters were taken using 5 nm passband filters with total exposure times of 12 hr and 14.7 hr, respectively. Reduction of these images detected considerable but very faint [O III] emission in addition to the nebula's already known $H\alpha$ emission. These data indicated the presence of even fainter [O III] emission farther out around the WR star plus hints of radial streamlines going from the nebula's inner region out to the edge of the faint extended [O III] emission.

These observations lead to much deeper images taken using a 0.60 m Planewave CDK24 telescope at the Ob-

servatorio El Sauce located in Rio Hurtardo Valley, Chile. These were taken using narrower 3 nm passband H α and [O III] $\lambda5007$ filters and a Moravian C3-61000 CMOS camera (9576 × 6388 pixels) yielding an image scale of 0'.'39 pix⁻¹ and a 20' × 13' FOV. Images were taken over 16 photometric and non-photometric nights in February and March 2024. Total exposure times in H α and [O III] were 9.3 hr (28 × 1200 s) and 16.3 hr (49 × 1200 s), respectively. Broadband R,G,B filter images were also obtained with single 20 minute exposures for each filter. These data were reduced using commercial imaging processing software including Pix-Insight and Astropixel Processor. A subset of these images were also reprocessed separately using a different set of software.

Additional images were obtained in late December 2024 using a 0.7 m Planewave CDK700 telescope also at Observatorio El Sauce in Chile. Using a Moravian C5-100 CMOS camera with 11664 \times 8750 pixels and 3 nm passband filters, images with total exposure times of 14.2 hr for H α and 19.2 hr for [O III] were obtained. These images were processed with Photoshop and Pix-Insight.

Lastly, as a check on some of the finer features of the WR 8's nebulosity, $\mathrm{H}\alpha + [\mathrm{N}\ \mathrm{II}]$ and $[\mathrm{O}\ \mathrm{III}]\ \lambda5007$ filter images were obtained in early January 2025 using the IMACS f/4.3 camera (Dressler et al. 2011) on the Baade 6.5m telescope at Las Campanas, Chile. This camera consists of a $8\mathrm{k}\times8\mathrm{k}$ mosaic covering an unvignetted field out to a radius of 12 arcmin. Three sets of 600 s exposures in each filter were taken offset from WR 8 and dithered so as to cover all the CCD chip gaps. Seeing during these observations ranged from 0.5" to 0.7". These data were processed by standard IMACS data reductions for mosaic imaging.

3. RESULTS AND DISCUSSION

Our H α and [O III] $\lambda5007$ images reveal a complex and striking nebulosity surrounding the bright WR 8 star, one that is far more extensive than previously realized. The images also show the presence of a faint halo of [O III] emission outside the nebula's main emission shell. Because of the nebula's extreme faintness, below we present the WR 8 nebula shown at different contrasts and brightness stretches to highlight various structural properties of the WR 8 nebula.

We begin with Figure 2 which shows our 0.6 m telescope $H\alpha$ and [O III] images of WR 8 nebula at low contrast so as to emphasize the similarity of the nebula's $H\alpha$ and [O III] line emissions as well as the relative brightnesses of various nebula features in these emission lines. Even at this low intensity display, the structure of the WR star's nebula seen in our in $H\alpha$ image is clearer and of higher resolution than that of the discovery SHS image (Fig. 1).

Although not commented on in the discovery paper by Stock & Barlow (2010), there is a relatively bright and

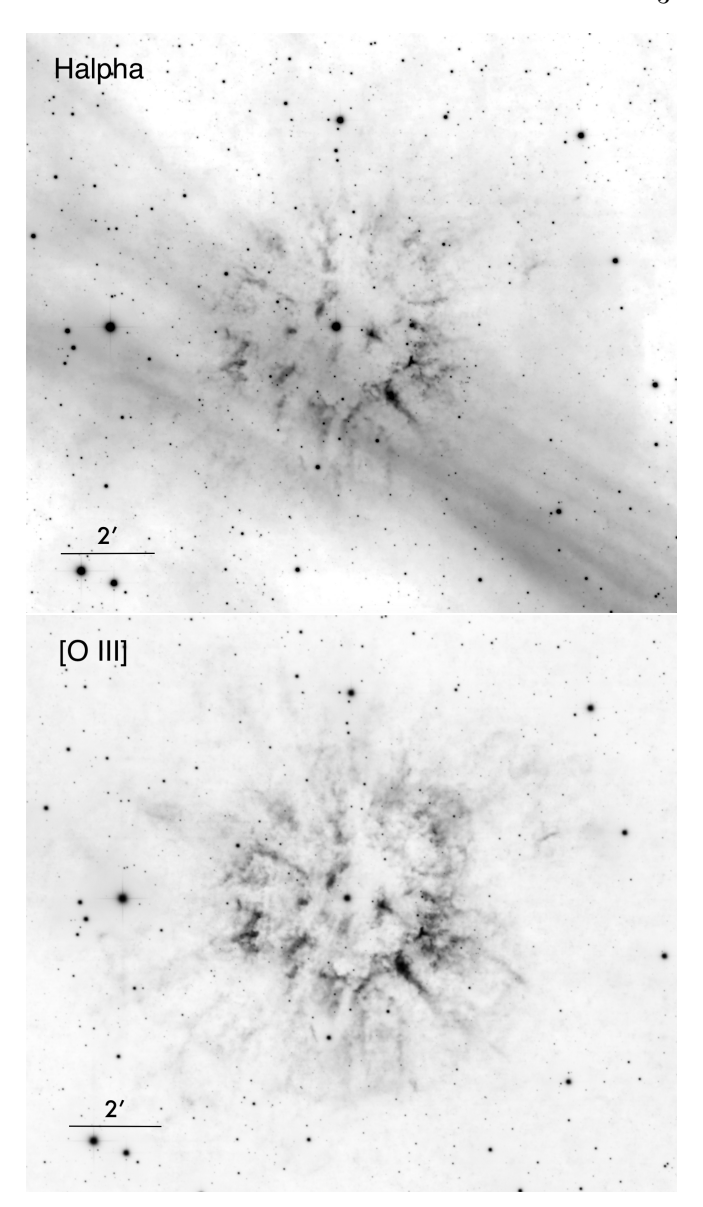


Figure 2. H α and [O III] images of the WR 8 nebula showing a comparison of the nebula's relative brightness in these line emissions. The broad band of diffuse emission seen in the H α image is unrelated background/foreground ISM emission. North is up, east to the left.

broad interstellar band of diffuse background or foreground H α emission that crosses over a large portion of the nebula's central and southern sections (see upper panel in Fig. 2). This emission complicates obtaining a clear picture of the nebula's full structure and prevents easy comparison of the nebula's H α vs. [O III] emission features and extent. (Note: This emission was noted by Marston et al. (1994a) and may have prevented them from noticing WR 8's faint nebula.)

Due to this overlapping $H\alpha$ emission, in the image presentations that follow, we emphasize the nebula's [O III]

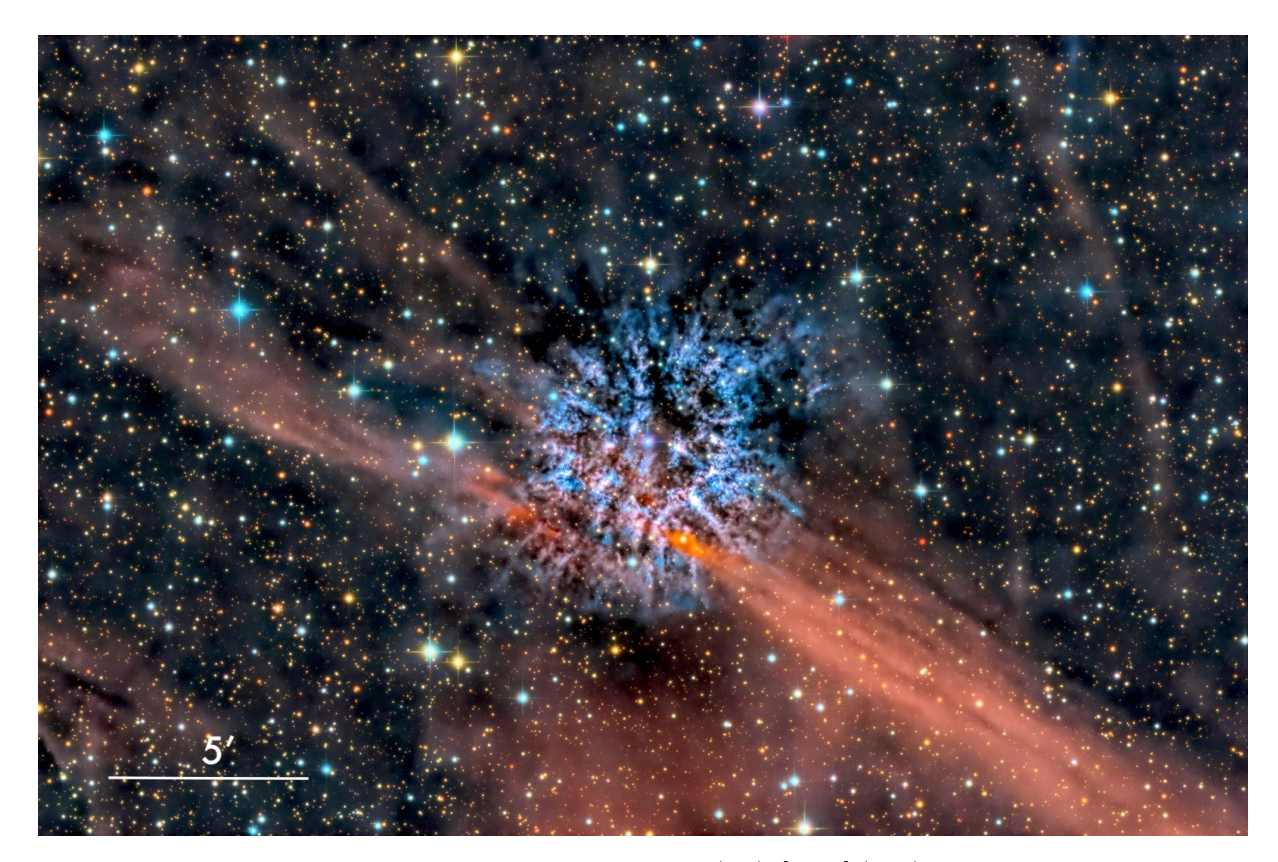


Figure 3. Wide FOV color image of WR 8 composited of $H\alpha$ (red), [O III] (blue) and broadband filter images.

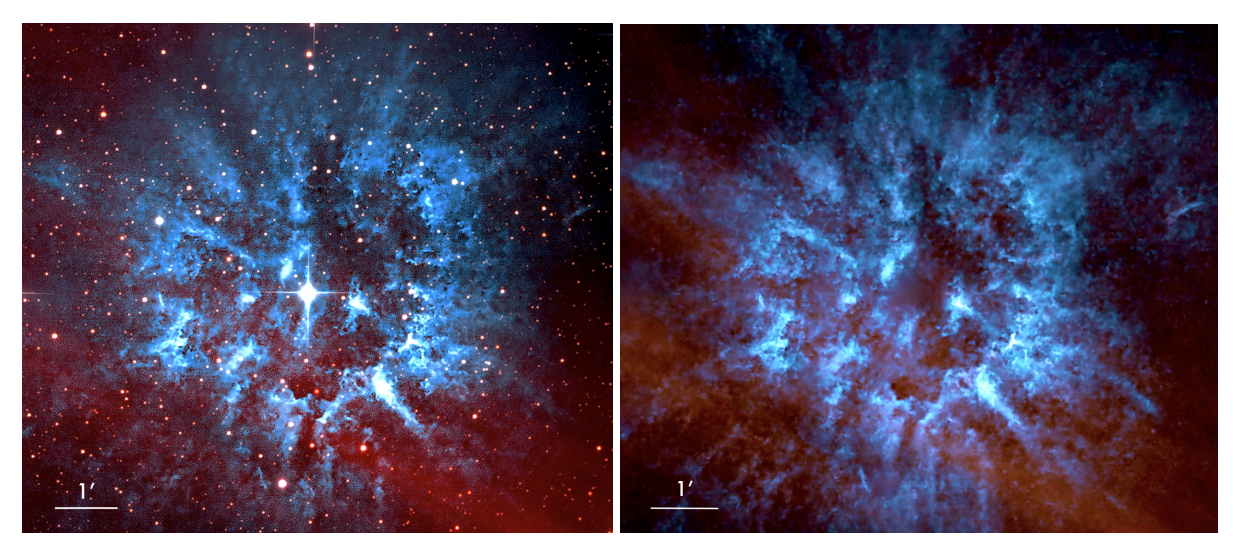


Figure 4. Two independent color composite $H\alpha$ and [O III] images of WR 8's nebula with and without stars.

emission structure over that seen in $H\alpha$ emission. In addition, because longer exposures were taken in the [O III] filter in all three of our image sets, this has led us to construct color composites suppressing $H\alpha$ relative to [O III] emissions. In these color composites, $H\alpha$ emission is shown as red while [O III] emission is blue. The result is the WR 8 nebula is shown with a strong blue color when, in fact, the nebula's [O III] is actually fainter than

that of its H α emission. Indeed, Stock et al. (2011) reported spectra that showed the nebula's [O III] emission much fainter than that of H α , with observed and extinction corrected F([O III] $\lambda 5007$)/F(H α) and I([O III] $\lambda 5007$)/I(H α) values of 0.22 and 0.79, respectively.

WR 8's nebulosity shown in Fig. 2 images may give the impression the WR 8 nebula is relatively bright when, in fact, it is quite faint. Based on its weak detection on

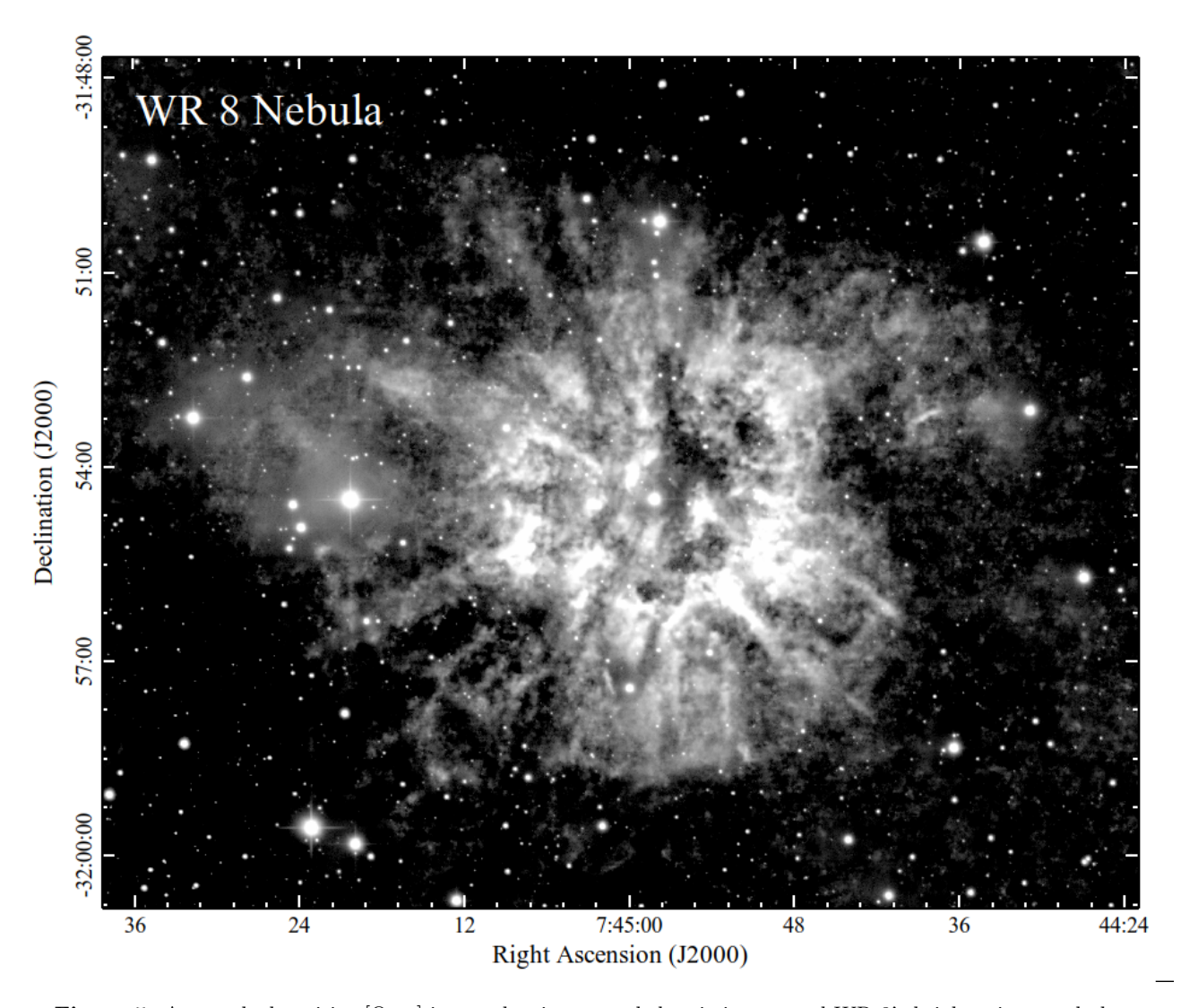


Figure 5. A stretched positive [O III] image showing extended emission around WR 8's brighter inner nebula.

SHS images at or near the estimated detection limit of that H α survey, specifically ≤ 5 Rayleighs¹, we estimate the nebula's H α to be roughly some 5 to 10 Rayleighs, corresponding to a H α flux of $\simeq 2.5-5\times 10^{-17}$ erg cm⁻² s⁻¹ arcsec⁻².

A wider view of the WR 8 nebula and interstellar emission along the line-of-sight is shown in Figure 3. This color $H\alpha$, [O III], and B,V,R filter composite of 0.6 m telescope images more clearly shows the broad interstellar band of $H\alpha$ emission along with the WR 8's nebula. The deeper [O III] images combined with the desire to present the nebula's structure without confusion of the overlapping band of interstellar $H\alpha$ emission leads to a color composite image showing a seemingly bright [O III] emission nebula.

The fine-scale structure of WR 8's nebula is better seen in the enlargements of Figure 4 where we show two independent color composite images. The left panel shows the nebula at the best resolution of our 0.7 m telescope data, while the right panel shows more of the nebula's fainter emission. Stars have been removed from the deeper right panel image using computer software in order to make the nebula's structure more readily visible. As noted above, the nebula's $H\alpha$ emission has been artificially suppressed compared to its [O III] emission, resulting in overlapping diffuse band of interstellar $H\alpha$ emission appearing only weakly in both panels.

Broadly, the nebula appears as a broken ring of numerous emission clumps the center of which is not exactly centered on the WR star, HD 62910. Extending out from this emission ring are several emission streaks and broad fans of emission extending some 1'-2' in length which fade with increasing radial distance. The nebula's brightest features are seen in the west-central and

 $^{^{1}}$ Rayleigh = $3.715 \times 10^{-14} \ \lambda^{-1} \ \mathrm{erg} \ \mathrm{cm}^{-2} \ \mathrm{s}^{-1} \ \mathrm{arcsec}^{-2}$

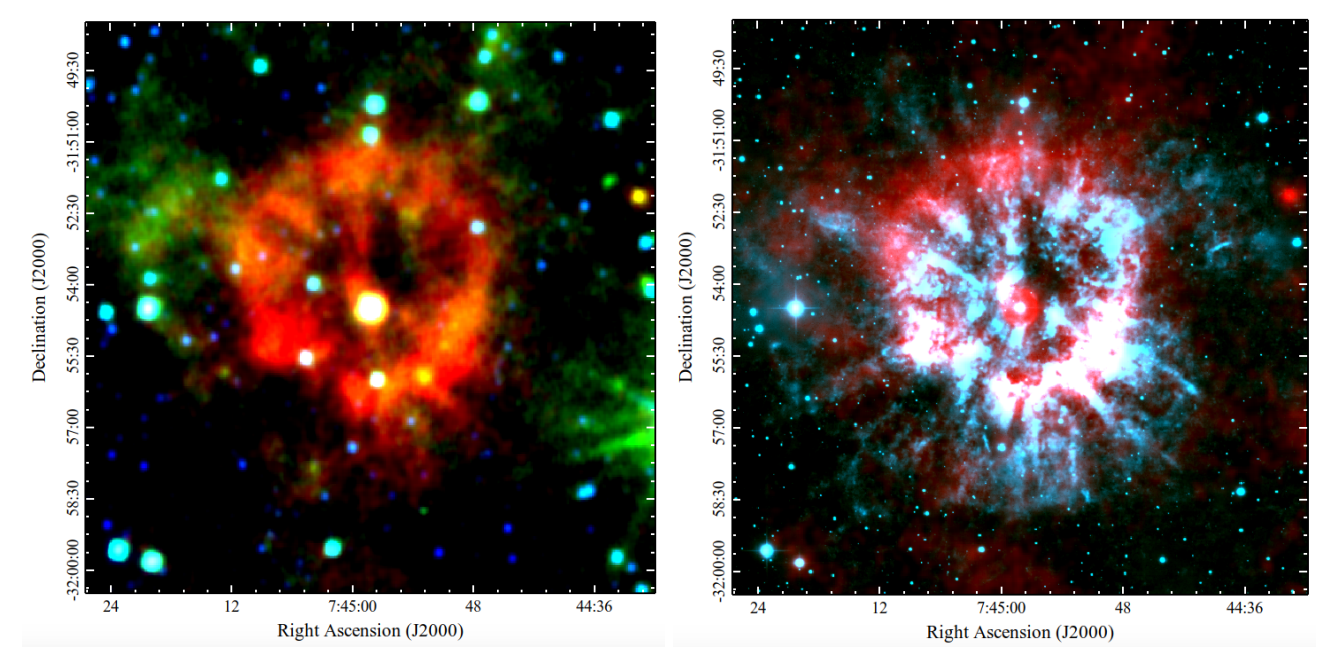


Figure 6. Color composites of WR 8's nebula. Left Panel: WISE 4.6 μ m (blue), 12 μ m (green), and 22 μ m (red) images. Right Panel: WISE 22 μ m (red) and [O III] λ 5007 (blue) images.

southwest areas along with some head-tail morphologies suggestive of wind sculptured clouds of stellar ejecta.

The appearance of the WR 8 nebula resembles that of the much brighter ejecta rich nebula RCW 58. Although having far fewer in number, it exhibits some of RCW 58 radial aligned streaks. However, unlike that seen for WR 8, RCW 58's nebula looks very different in ${\rm H}\alpha$ where it is highly clumpy compared to its [O III] emission where the nebula much more diffuse with fewer clumpy features.

In contrast, WR 8's morphology is about the same in $H\alpha$ and [O III]. Also, whereas most of RCW 58's nebula is concentrated in its outer regions with a relatively clear central region, WR 8's nebula has more inner emission clouds. In this respect, it resembles somewhat the cloudy M1-67 nebula although having far few clouds. Finally, based upon their similar appearances on SHS images, the faint and recently recognized WR 71 nebula shares some structural features including an incomplete and clumpy shell (Marston et al. 1994b; Stock & Barlow 2010).

Figure 5 shows a stretched version of our deepest $[O\ III]$ image in order to show the nebula's outermost extent. Whereas the bright inner emission ring spans some 5'-6' in diameter, the nebula's outermost regions have N-S and E-W dimensions around 9' and 13', respectively. Much of the nebula's southern sections appear to have a well defined boundary some 4.3' from the WR star. But that is not the situation for the other outer emission regions, especially to the east where a large diffuse patch of $[O\ III]$ emission is seen. This ex-

tended outer and more diffuse emission is perhaps due to a lower mass loss rate episode in WR 8's history.

Due to the strong overlapping interstellar band of $H\alpha$ emission one cannot determine if the nebula's outer regions looks the same as that seen in [O III]. What is clear, however, is that the nebula exhibits a somewhat similar clumpy but yet different appearance in the infrared from that seen in optical line emissions.

As noted by Toalá et al. (2015), WR 8 possesses a bright nebular ring at 22 μ m. This can be seen in the left panel of Fig. 6 where we combined WISE blue 4.6 μ m, green 12 μ m, and red 22 μ m images into a color composite of the WR 8 nebula. Much like that seen in the optical, this infrared emission mainly due to thermal continuum emission from dust (Toalá et al. 2015) shows a fairly clumpy emission structure but in a better defined shell. The geometric center of this shell lies some 40" north of ER 8, making the star appear noticeably off-center.

The right hand panel of Fig. 6 shows a color composite of our [O III] $\lambda5007$ image in blue with the WISE 22 $\mu{\rm m}$ image in red. The clumpy structure seen in the infrared image is seen to be associated with many of the clumpy features in our [O III] emission images, especially along the nebula's northern rim. However, the gross morphology differences between WR 8's infrared nebula and its [O III] emissions indicate differences of where WR 8's nebula's thermal dust emission lies vs. its ionized gas.

Unlike the general similarity found by Toalá et al. (2015) for H α and 22 μ m emissions in most WR ring nebulae, WR 8's nebula appears especially noticeably

WR	Nebula	Wolf-Rayet	Spectral	Nebula Diameter	Distance a	Physical Size	References
Name	Name	Star	Type	(arcmin)	(kpc)	(pc)	
WR 6	S308	$\mathrm{HD}\ 50896$	WN4	40	1.51 ± 0.09	17.6	1, 2, 3
WR 8		$^{ m HD}$ 62910	WN6/WC4	6	3.52 ± 0.16	6.1	1, 4
WR 40	RCW 58	HD 96548	WN8	7×9	2.70 ± 0.12	$5.5~\mathrm{x}~7.1$	5
WR 71		HD 143414	WN6	4	4.27 ± 0.39	5.0	1, 6
WR 124	M1-67	BAC 209	WN8	1.2	5.36 ± 0.38	1.9	5

Table 1. Comparison of Some Ejecta Rich Wolf-Rayet Nebulae

WN6

References: 1) Stock & Barlow (2010); 2) Esteban et al. (1992); 3) Chu et al. (2003); 4) this paper; 5) Chu et al. (1983); 6) Marston et al. (1994b); 7) Chu (1991) 8) Esteban & Vilchez (1992)

 12×18

 1.67 ± 0.04

different along the [O III] clumps and streamers along its northern rim. Whereas the nebula's warm dust as detected in the 22 $\mu \rm m$ image lies coincident with WR 8's bright optical features in south, its 22 $\mu \rm m$ emission is mainly seen in the fainter outer portions of bright [O III] northern emission clumps. It is this greater radial distance of dust emission along the nebula's northern areas that is responsible for the striking off-center position of the WR star from the middle of the IR shell. We further note that a stronger intensity stretch of the 22 $\mu \rm m$ image shows fainter IR emission surrounding much of this otherwise well defined shell, especially to the south and southwest which is coincident with some very faint [O III] emission.

WR 136

NGC 6888

HD 192163

The cause for the stark coincidence difference of the nebula's dust in and around the nebula's ionized gas clumps in the south compared to what is seen in the north is unclear. Our [O III] images show considerably more and brighter emission in the south compared to the north (see Figs. 2 and 4), raising the possibility of differential dust temperatures in the north vs. south assuming a constant gas to dust ratio. Greater gas densities and optical depths in gasous clumps located along the shell's southern rim might give rise to cooler dust relative to warmer dust in the less dense and less UV shielded northern regions. However, this might not explain the weak infrared emission for some of the nebula's other optically bright features such as in its east-central region.

Finally, one can ask how does WR 8's nebula's physical size compare to other ejecta dominated ring nebula. In Table 1, we list the WR 8's nebula compared to several WR ring nebula rich in stellar ejecta indicated by over-abundances of nitrogen and helium as markers of the CNO process of energy production in high mass stars. One sees that this small and select group of Etype WR nebulae have fairly similar physical diameters

of around 5 to 15 pc. Although WR 6's S308 nebula is the largest of this group, WR 8 nebula's faint outer angular dimensions of $9' \times 13'$ corresponding to roughly 9×14 pc is not that far behind. We note that the M1-67 nebula stands out from the rest as the smallest, presumably due to its younger age.

 5.8×8.7

1, 5, 7, 8

Thus it seems that WR 8's nebula as detected in our images is not unlike those of other ejecta rich WR nebulae. While Stock et al. (2011) did not report on the expansion velocity of WR 8's nebula. if we choose an expansion velocity like that seen for other WR nebulae, namely of order 60 km s⁻¹ (Smith 1994; Sirianni et al. 1998), then the \simeq 3 pc radius of its bright main shell suggests a dynamical age of around 50 kyr.

In summary, our optical line emission images show WR 8 to possess a striking and extensive optical nebula consisting of a brighter inner ring of emission surrounded by an outer nebula of fainter emission best seen in [O III]. Overall, the WR 8 nebula is especially visually impressive compared to many other WR ring nebulae. Being one of only a few WR stars having a stellar ejecta dominated nebula and being associated with a WR star in transition from WN to WC, its nebula deserves further study. An in depth spectral investigation of its main shell and outer halo of emission may prove helpful in improving our understanding of the brief WN to WC transition phase.

We would like to thank Phil Massey for encouraging our imaging of WR 8, an anonymous referee for several helpful suggestions, and Yuri Beletsky of Las Campanas Observatory for help obtaining the IMACS observations on WR 8. This work is part of R.A.F's Archangel III Research Program at Dartmouth.

Facilities: Las Campanas Observatory, Observatorio El Sauce, Chile

^aDistances are Bayesian corrected geometric values from Bailer-Jones et al. (2021) for Gaia DR3.

Software: Photoshop, PixInsight, Astropixel Processor, DS9 fits viewer Joye & Mandel (2003), WCSTools Laycock et al. (2010)

REFERENCES

- Abbott, D. C. 1982, ApJ, 263, 723, doi: 10.1086/160544
 Abbott, D. C., & Conti, P. S. 1987, ARA&A, 25, 113, doi: 10.1146/annurev.aa.25.090187.000553
- Bailer-Jones, C. A. L., Rybizki, J., Fouesneau, M., Demleitner, M., & Andrae, R. 2021, AJ, 161, 147, doi: 10.3847/1538-3881/abd806
- Chu, Y. H. 1981, ApJ, 249, 195, doi: 10.1086/159275
- Chu, Y. H. 1991, in IAU Symposium, Vol. 143, Wolf-Rayet Stars and Interrelations with Other Massive Stars in Galaxies, ed. K. A. van der Hucht & B. Hidayat, 349
- Chu, Y.-H. 2016, in Journal of Physics Conference Series, Vol. 728, Journal of Physics Conference Series (IOP), 032007, doi: 10.1088/1742-6596/728/3/032007
- Chu, Y.-H., Guerrero, M. A., Gruendl, R. A., García-Segura, G., & Wendker, H. J. 2003, ApJ, 599, 1189, doi: 10.1086/379607
- Chu, Y. H., Treffers, R. R., & Kwitter, K. B. 1983, ApJS, 53, 937, doi: 10.1086/190914
- Conti, P. S. 2000, PASP, 112, 1413, doi: 10.1086/317693
 Conti, P. S., & Massey, P. 1989, ApJ, 337, 251, doi: 10.1086/167101
- Crowther, P. A. 2007, ARA&A, 45, 177, doi: 10.1146/annurev.astro.45.051806.110615
- Crowther, P. A. 2008, in IAU Symposium, Vol. 250, Massive Stars as Cosmic Engines, ed. F. Bresolin, P. A. Crowther, & J. Puls, 47–62, doi: 10.1017/S1743921308020334
- Deshmukh, K., Sana, H., Mérand, A., et al. 2024, A&A, 692, A109, doi: 10.1051/0004-6361/202452352
- Dressler, A., Bigelow, B., Hare, T., et al. 2011, PASP, 123, 288, doi: 10.1086/658908
- Esteban, C., Mesa-Delgado, A., Morisset, C., & García-Rojas, J. 2016, MNRAS, 460, 4038, doi: 10.1093/mnras/stw1243
- Esteban, C., & Vilchez, J. M. 1992, ApJ, 390, 536, doi: 10.1086/171303
- Esteban, C., Vilchez, J. M., Smith, L. J., & Clegg, R. E. S. 1992, A&A, 259, 629
- Hamann, W. R., Gräfener, G., Liermann, A., et al. 2019, A&A, 625, A57, doi: 10.1051/0004-6361/201834850
- Heckathorn, J. N., Bruhweiler, F. C., & Gull, T. R. 1982, in IAU Symposium, Vol. 99, Wolf-Rayet Stars:
 Observations, Physics, Evolution, ed. C. W. H. De Loore & A. J. Willis, 463
- Hillier, D. J., Aadland, E., Massey, P., & Morrell, N. 2021, MNRAS, 503, 2726, doi: 10.1093/mnras/stab580

- Johnson, H. M., & Hogg, D. E. 1965, ApJ, 142, 1033, doi: 10.1086/148373
- Joye, W. A., & Mandel, E. 2003, in Astronomical Society of the Pacific Conference Series, Vol. 295, Astronomical
 Data Analysis Software and Systems XII, ed. H. E.
 Payne, R. I. Jedrzejewski, & R. N. Hook, 489
- Kwitter, K. B. 1984, ApJ, 287, 840, doi: 10.1086/162742
- Laycock, S., Tang, S., Grindlay, J., et al. 2010, AJ, 140, 1062, doi: 10.1088/0004-6256/140/4/1062
- Maeder, A., & Conti, P. S. 1994, ARA&A, 32, 227, doi: 10.1146/annurev.astro.32.1.227
- Marchenko, S. V., Moffat, A. F. J., Eversberg, T., et al. 1998, MNRAS, 294, 642, doi: 10.1111/j.1365-8711.1998. 01174.x10.1046/j.1365-8711.1998.01174.x
- Marston, A. P., Chu, Y. H., & Garcia-Segura, G. 1994a, ApJS, 93, 229, doi: 10.1086/192053
- Marston, A. P., Yocum, D. R., Garcia-Segura, G., & Chu, Y. H. 1994b, ApJS, 95, 151, doi: 10.1086/192097
- Niemela, V. S. 1991, in IAU Symposium, Vol. 143, Wolf-Rayet Stars and Interrelations with Other Massive Stars in Galaxies, ed. K. A. van der Hucht & B. Hidayat, 201
- Oey, M. S. 1999, in IAU Symposium, Vol. 193, Wolf-Rayet Phenomena in Massive Stars and Starburst Galaxies, ed. K. A. van der Hucht, G. Koenigsberger, & P. R. J. Eenens, 627
- Parker, Q. A., Phillipps, S., Pierce, M. J., et al. 2005, MNRAS, 362, 689, doi: 10.1111/j.1365-2966.2005.09350.x
- Sander, A., Hamann, W. R., & Todt, H. 2012, A&A, 540, A144, doi: 10.1051/0004-6361/201117830
- Sander, A. A. C., Vink, J. S., Higgins, E. R., et al. 2022, in IAU Symposium, Vol. 366, The Origin of Outflows in Evolved Stars, ed. L. Decin, A. Zijlstra, & C. Gielen, 21–26, doi: 10.1017/S1743921322000400
- Sirianni, M., Nota, A., Pasquali, A., & Clampin, M. 1998, A&A, 335, 1029
- Smith, L. J. 1994, Ap&SS, 216, 291, doi: 10.1007/BF00982507
- Stock, D. J., & Barlow, M. J. 2010, MNRAS, 409, 1429, doi: 10.1111/j.1365-2966.2010.17124.x
- —. 2014, MNRAS, 441, 3065, doi: 10.1093/mnras/stu724
- Stock, D. J., Barlow, M. J., & Wesson, R. 2011, MNRAS, 418, 2532, doi: 10.1111/j.1365-2966.2011.19643.x

Toalá, J. A., Guerrero, M. A., Ramos-Larios, G., & Guzmán, V. 2015, A&A, 578, A66, doi: 10.1051/0004-6361/201525706

van der Hucht, K. A. 2001, NewAR, 45, 135, doi: 10.1016/S1387-6473(00)00112-3

van der Hucht, K. A., Conti, P. S., Lundstrom, I., & Stenholm, B. 1981, SSRv, 28, 227, doi: 10.1007/BF00173260

Wachter, S., Cohen, M., & Leisawitz, D. 2011, in American Astronomical Society Meeting Abstracts, Vol. 217, 333.10 Willis, A. J., & Stickland, D. J. 1990, A&A, 232, 89